

# Probing Ionospheric Structures Using LOFAR

M.Mevius  
on behalf of the LOFAR EOR team

**ASTRON**



**European Research Council**

Established by the European Commission

**Supporting top researchers  
from anywhere in the world**

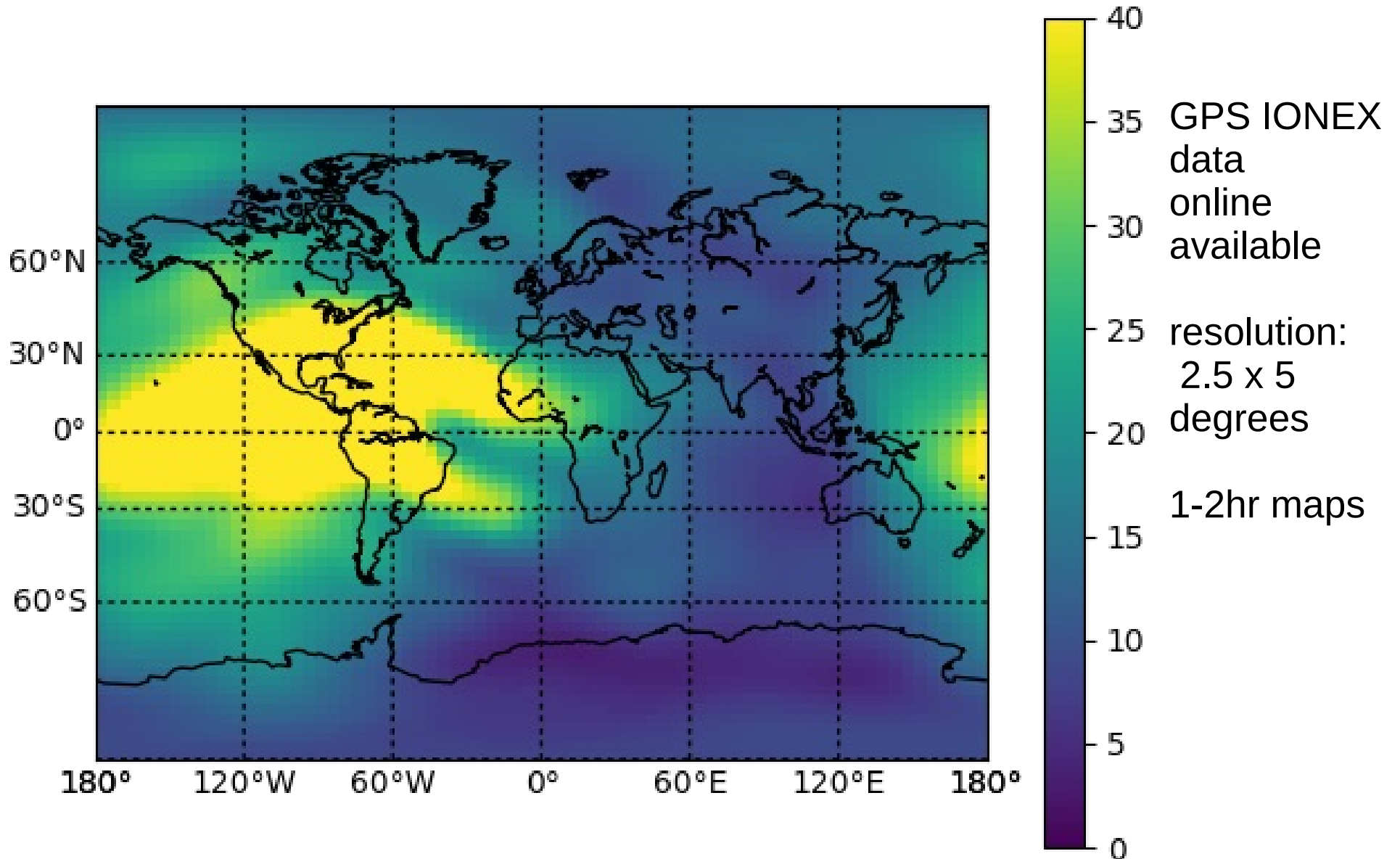


**LOFAR**

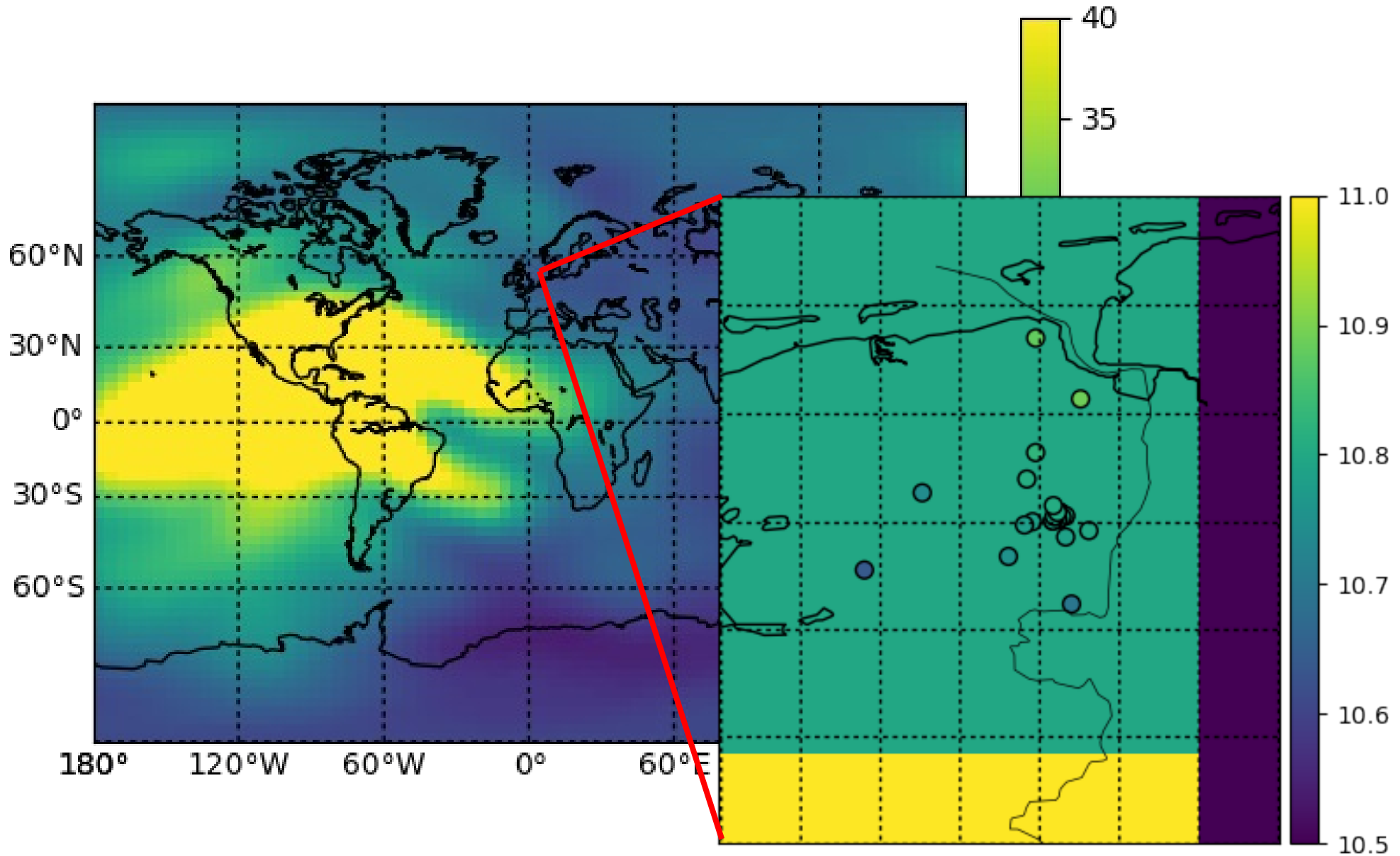
# OUTLINE

- LOFAR as ionospheric instrument
- Using Calibration solutions
- Structure Function
- Anisotropy
- Imaging ionospheric Structures

# LOFAR vs GPS



# LOFAR vs GPS



# NEW ILTG maps: See poster by Kotulak et.al,



## Implementation of ILT dedicated regional ionosphere maps to the low frequency radio observations

Kacper Kotulak<sup>1</sup>, Adam Fron<sup>1</sup>, Andrzej Krankowski<sup>1</sup>, Maaijke Mevius<sup>2</sup>, Manuel Hernández-Pajares<sup>3</sup>, Richard Fallows<sup>2</sup>, Biagio Forte<sup>4</sup>, Mario Bisi<sup>5</sup>, Leszek Blaszkiewicz<sup>1,6</sup>, Bartosz Dąbrowski<sup>1</sup>, Marcin Hajduk<sup>1</sup>, Tomasz Sidorowicz<sup>1</sup>

<sup>1</sup>Space Radio-Diagnostics Research Centre, University of Warmia and Mazury, Olsztyn, Poland  
<sup>2</sup>ASTRON - Netherlands Institute for Radio Astronomy, Netherlands  
<sup>3</sup>Ionospheric determination and Navigation based on Satellite And Terrestrial systems research team (IONSAT), Universitat Politècnica de Catalunya (UPC), Spain  
<sup>4</sup>Department of Electronic and Electrical Engineering, University of Bath, England  
<sup>5</sup>RAL Space, Science & Technology Facilities Council - Rutherford Appleton Laboratory, Harwell, Oxford, England  
<sup>6</sup>Chair of Relativistic Physics, Faculty of Mathematics and Computer Science, University of Warmia and Mazury, Olsztyn, Poland



### Introduction

The high spatial and temporal resolution ionospheric products dedicated to the International LOFAR Telescope (ILT) purposes are produced in a result of arrangements made during 2016 LOFAR Ionospheric Workshop in Warsaw. The main idea is to introduce product that would replace the currently used global maps with improvement of the accuracy. The proposed product is based on the total electron content map (TEC) adjusted to the operational area of the ILT (34N to 55N in latitude and 11W to 25E in longitude) with the resolution of 0.5 degree. As for temporal resolution, two types of products are introduced: ILTF - five minutes averaged map and ILTQ - fifteen minutes averaged map. Maps are generated using information about the total electron content from the GNSS observations performed by 126 EUREF Permanent Network (EPN) stations. Obtained TEC values are computed into corresponding vertical values and interpolated into target grid using natural neighbour interpolation technique. ILTF and ILTQ products' validity performs well when compared to the other GNSS-based ionospheric products and the radar altimeter JASON measurements and show noticeable accuracy improvement of the Faraday rotation observation with the LOFAR telescope. ILT IONEX files since 2012 are available via the dedicated ftp server.

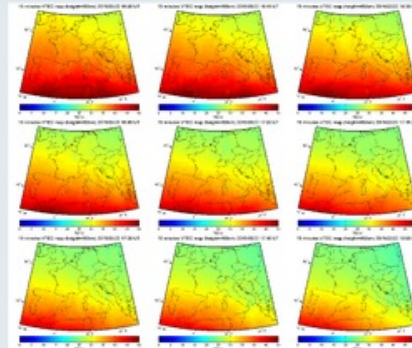


Fig. 3 ILTQ maps temporal and spatial resolution for 16:00-18:00 UT, March 22 2017

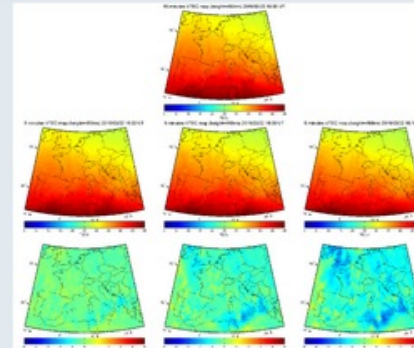


Fig. 4 ILTQ map compared to corresponding respective ILTF maps

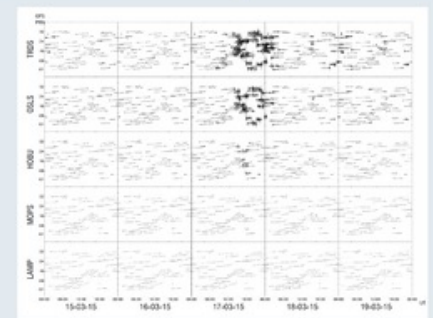


Fig. 8 ROT index for St. Patrick's Day storm (on the event day, two days before and two days after) for observations from five stations with latitudinal span from 63°N to 36°N (TEC 63°N, OLS 59°N, HOBU 53°N, MOPS 44°N and LAMP 35°N).

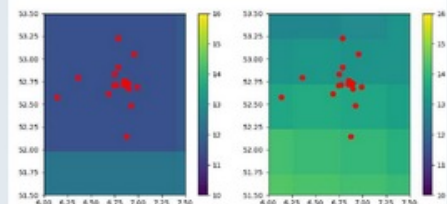


Fig. 1 Ionospheric products (IGSG on the left and ILTQ on the right) above Dutch part of LOFAR

### GPS-based ionosphere maps

For years, the GNSS permanent station observation data were used in monitoring the state of ionosphere. By combining the dual-frequency measurements of permanent GNSS receivers it is possible to obtain information about the state of the ionosphere (Schaer, 1999).

GNSS ionospheric maps are used for example for estimating ionospheric component in calibration of Faraday rotation measurements (Sotomayor-Beltran, et al., 2013). However such elaboration use global ionospheric maps with spatial resolution of 5 degrees in longitude, 2.5 degrees in latitude and 2 hours temporal resolution.

ILTQ and ILTF products are elaborated in response to that problem.

Figure 2 shows spatial and temporal resolution for IGSG product for time interval 16:00-18:00UT on March 22 2015. Figure 3 presents ILTQ maps for the same period. Spatial and temporal (nine maps depicting 2-hour period instead of two) resolution improvement can be clearly seen. Figure 4 shows difference between 15-minute (ILTQ - upper panel) and 5-minute (ILTF - middle panel) products - the bottom panel contains differences between ILTQ maps and respective corresponding ILTFs.

Figure 5 and table 1 present validity of ILTQ product and accuracy improvement in regard to other products.

GIM id	Std. Dev. / TECU	Bias / TECU	RMS / TECU	Rel. Err. / %
ILTQ	1.46	-0.95	2.16	13.7
IGSG	1.62	-1.65	2.61	16.3
COGS	1.65	-1.04	2.45	15.6
ESAG	1.87	-0.74	2.58	16.3
JPLG	1.63	-2.94	3.50	21.6
LPCG	1.54	-0.95	2.24	14.1

Table 1: Summary of the performance of new ILTQ, IGSG and LQCG GIMs versus JASON VTEC on the European seas, since 2012 to 2016.

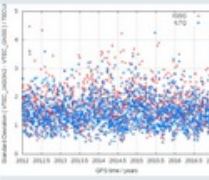


Fig. 5: Standard deviation of the JASON - GIM VTEC for IGSG (red points) and ILTQ (blue points) during years 2012-2016.

### Ionosphere influence on LOFAR

Despite its obvious influence, ionospheric effects in low-frequency observations have usually been discounted due to the poor resolution and sensitivity of instruments, lack of computer power or satisfying performance of calibration algorithms like self-calibration (Intema et al., 2009). In regard to LOFAR many authors point that ionosphere influence calibration is crucial and cannot be ignored (e.g. van der Tol and van der Veen, 2007). It is one of the main calibration steps of LOFAR, ionospheric effects are stronger on low frequencies because ionospheric phase shift scales with the wavelengths (van der Tol and van der Veen, 2007).

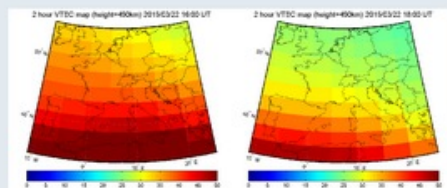


Fig. 2 IGSG maps temporal and spatial resolution for 16:00-18:00 UT, March 22 2017



Fig. 6: EPN stations used in TEC (blue dots) and ROT (red dots) elaboration.

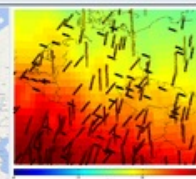


Fig. 7: Exemplary set of ionospheric Pierce Points over central Europe collected over 15 minutes and

### Ionospheric fluctuation indices

To describe ionospheric irregularities special indices are incorporated. First fluctuation measure is rate of TEC (ROT) which illustrates variability of the total electron content in time within each satellite trajectory.

ROT is then highly dependent on the line of sight between satellite and receiver and fluctuates around small value. To achieve statistically better measure, rate of TEC index (ROTI) was introduced. ROTI is based on the standard deviation of the ROT.

### Fluctuation products

Presented fluctuation product was created in reference to newly introduced to International GNSS Service (IGS) global fluctuation product (Chemiak et al. 2014). Presented elaboration uses the same area as ILTF/ILTQ maps. However, no interpolation techniques have been incorporated, thus not whole area is actually covered. 189 EPN stations observations are used in elaboration. ROTI is calculated in 2 by 2 degrees boxes with 5 minutes of averaging time.

### References:

Intema H.T., van der Tol S., Cotton W.D., Cohen A.S., van Bommel, I.M., Rottgering H.J.A. (2009), Ionospheric calibration of low frequency radio interferometric observations using the peeling scheme van der Tol S., van der Veen A.-I. (2007), Ionospheric calibration for the LOFAR Radio Telescope Gaussian II T.L., Bust G.S., Garner T.W. (2004), LOFAR as an ionospheric probe Sotomayor-Beltran C. et al. (2013), Calibrating high-precision Faraday rotation measurements for LOFAR and the next generation of low-frequency radio telescopes I. Chemiak, A. Krankowski, I. Zakharenkova (2014) Observation of the ionospheric irregularities over the Northern Hemisphere: Methodology and service

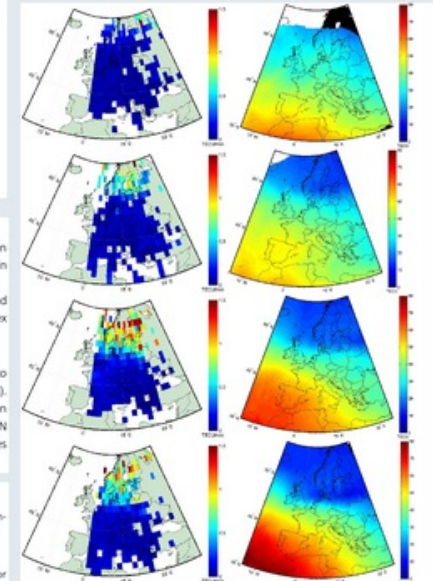
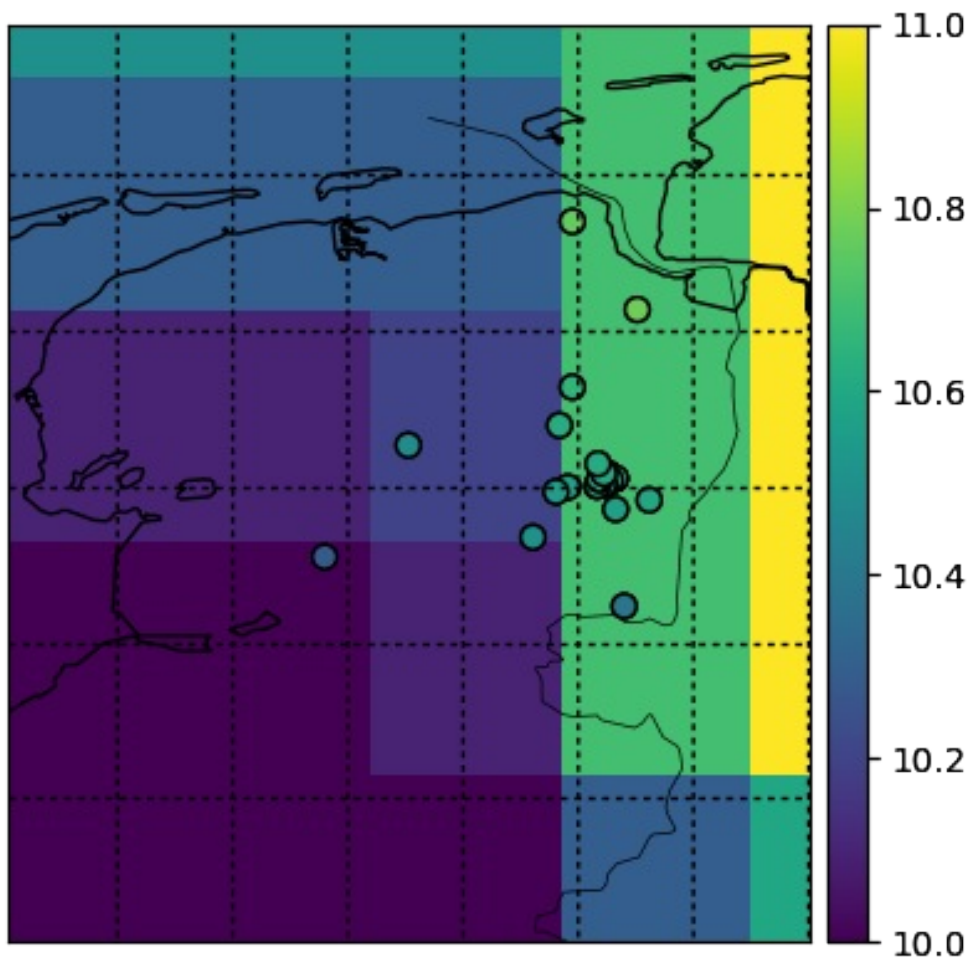


Fig. 9: Maps presenting ROTI (left panel) and TEC (right panel) in the beginning of St. Patrick's Day 2015 storm (17.03.2015) - for epochs 14:00 UT, 15:00 UT, 16:00 UT, 17:00 UT.





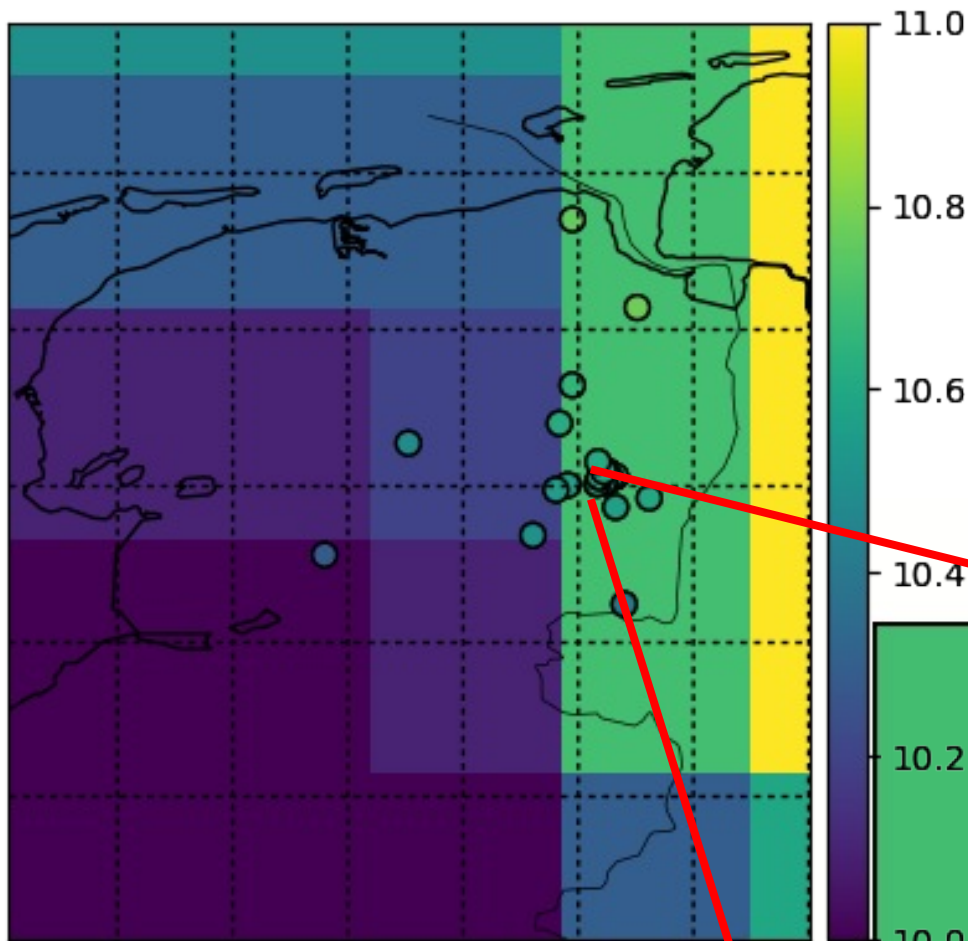
High resolution GPS  
vTEC maps

0.5 x 0.5 degrees

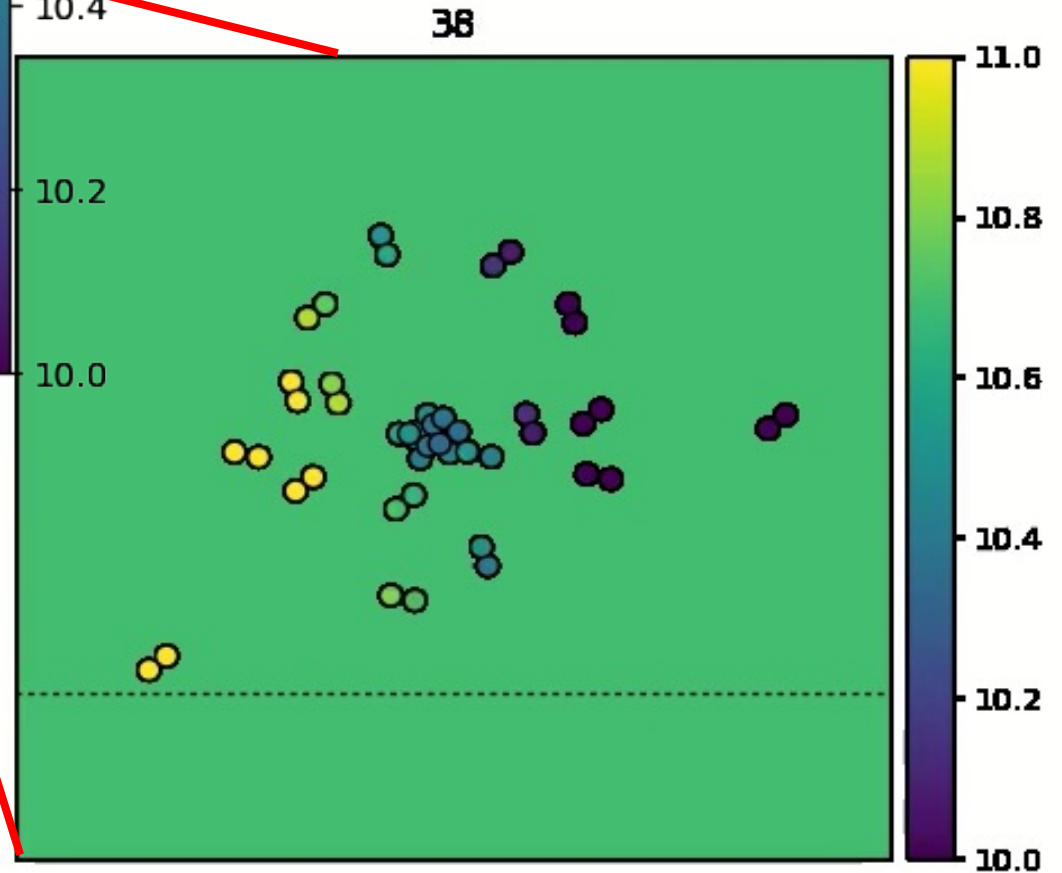
time resolution:  
5min/15min

Uncertainty  $\sim 1$ TECU  
(corresponds to  $\sim 4$  full  $2\pi$   
phase rotations @ LOFAR  
HBA)

Faraday rotation correction of polarized signals  
precalibration of International baselines  
absolute TEC measurements



LOFAR CS: dTEC solutions with a time resolution of 10 s  
Colorscale ranges from **-0.005 to 0.005 TECU**



For even higher time resolution see presentation by Richard Fallows

# Calibration Solutions

- Ionosphere is a major issue for the calibration of low frequency data
- Calibration solutions provide information about ionosphere
- Ionospheric characterization tool for quality assignment of radio data

In this presentation:  
LOFAR-EOR 3C196 data  
Direction independent  
calibration using 4  
component model of 3C196  
Analyze full Jones matrices  
Snapshot imaging



**Phase error:**

$$\Phi^{\text{ion}} = -\frac{2\pi\nu}{c} \int_{\text{LoS}} (n - 1) dl$$

**Refractive index expansion:**

$$n = 1 - \frac{q^2}{8\pi^2 m_e \epsilon_0} \cdot \frac{n_e}{\nu^2} \pm \frac{q^3}{16\pi^3 m_e^2 \epsilon_0} \cdot \frac{n_e B \cos \theta}{\nu^3} - \frac{q^4}{128\pi^4 m_e^2 \epsilon_0^2} \cdot \frac{n_e^2}{\nu^4} - \frac{q^4}{64\pi^4 m_e^3 \epsilon_0} \cdot \frac{n_e B^2 (1 + \cos^2 \theta)}{\nu^4}$$

dTEC (TECU)	I ord 30 MHz	II ord (day/night) 30 MHz	I ord 60 MHz	II ord (day/night) 60 MHz	I ord 150 MHz	II ord (day/night) 150 MHz
0.5 (remote st., bad iono.)	8067	294 / 214	4033	73 / 50	1613	12 / 8
0.1 (remote st., good iono.)	1613	126 / 46	806	31 / 10	322	5 / 2
0.03 (across FoV)	404	97 / 16	242	24 / 4	96	4 / < 1
0.01 (core st.)	160	88 / 8	80	22 / 2	31	4 / < 1

Calibration: in M.E., Jones matrices:

$$\alpha = \text{RM} \cdot \lambda^2$$

$$\begin{pmatrix} G_{xx} & G_{xy} \\ G_{yx} & G_{yy} \end{pmatrix} = \begin{pmatrix} \cos(\alpha) & \sin(\alpha) \\ -\sin(\alpha) & \cos(\alpha) \end{pmatrix} \cdot \begin{pmatrix} G_{xx} & 0 \\ 0 & G_{yy} \end{pmatrix}$$

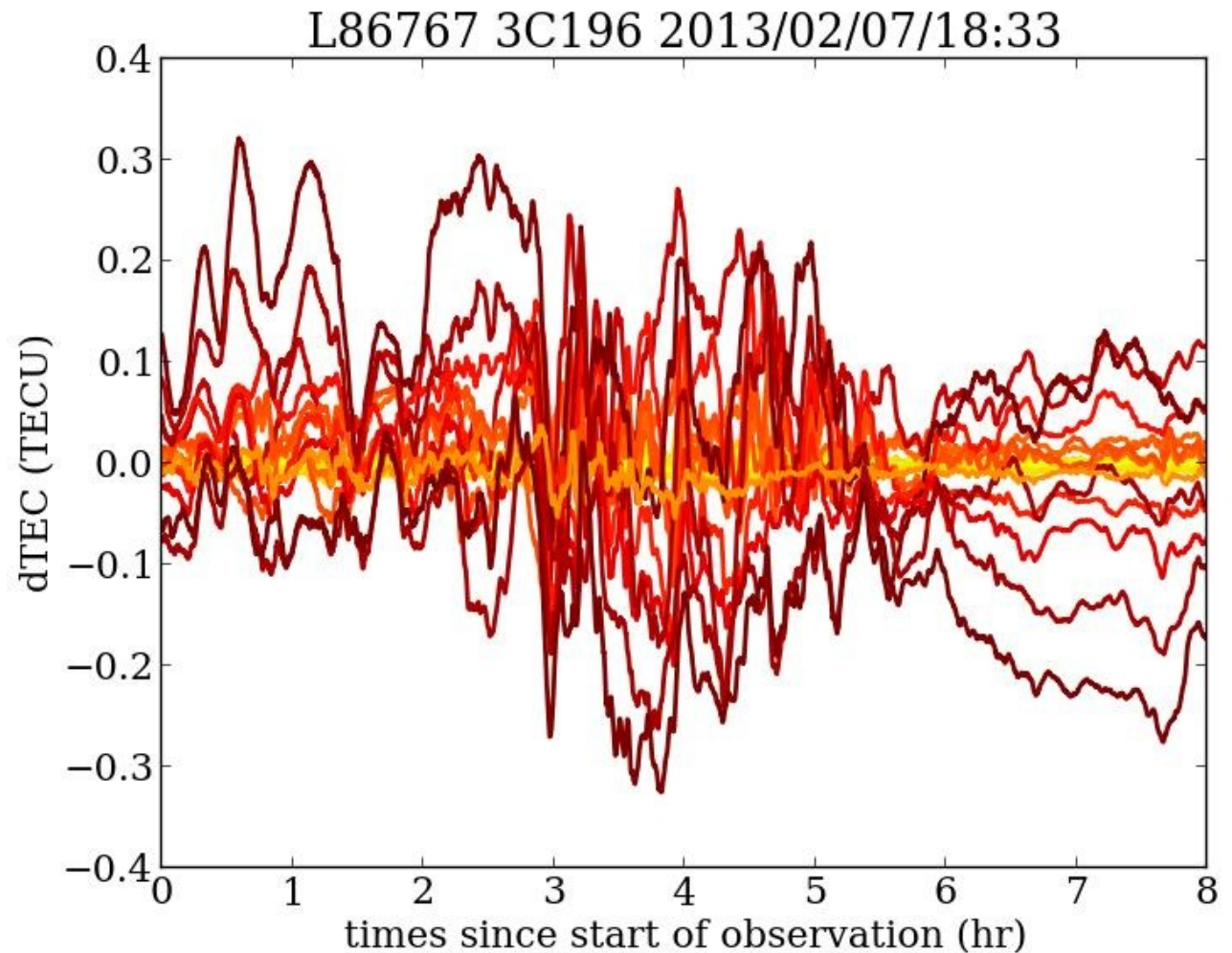
After clock-TEC  
separation:

## dTEC vs. time

each line corresponds to a  
different baseline (wrst center  
LOFAR)  
darker colors correspond to  
longer baselines

LOFAR HBA data  
(115-170 MHz)  
4 component model of  
calibrator (3C196) in phase  
center

solution every 10s



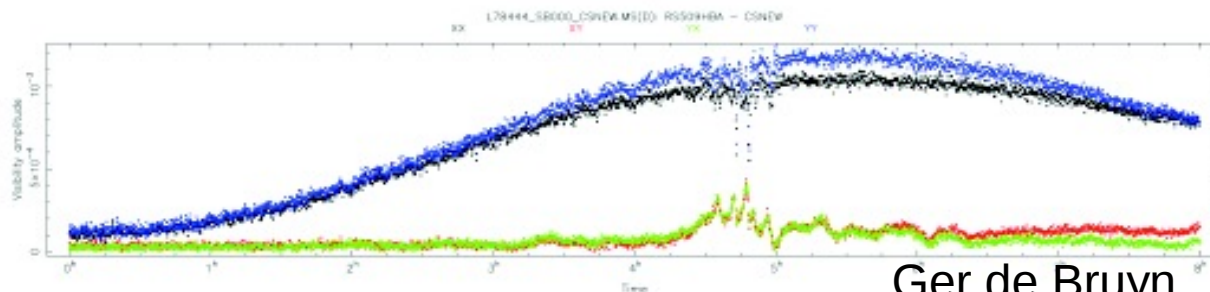
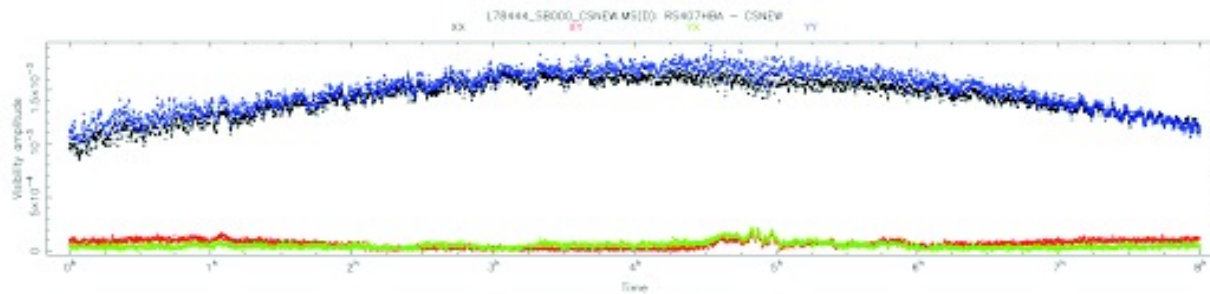
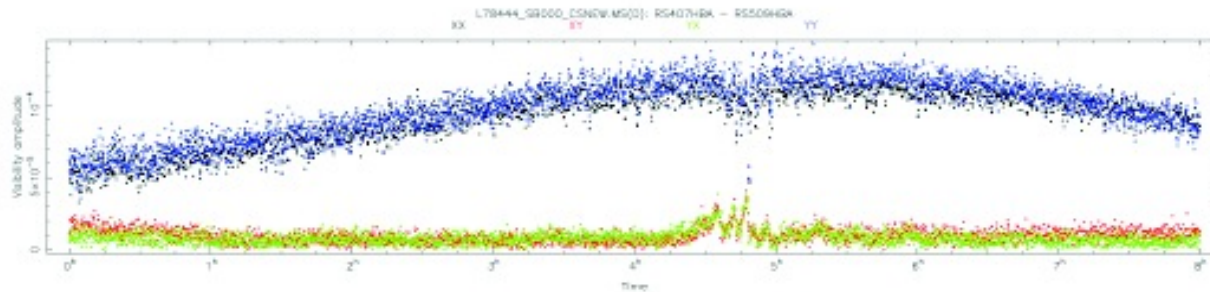
(almost) independent fit for each time point!

estimated accuracy from scatter round trend  
(calibrator data):

dTEC:  $< 0.001$  TECU

# 2<sup>nd</sup> order: Differential Faraday rotation

$$\begin{pmatrix} G_{xx} & G_{xy} \\ G_{yx} & G_{yy} \end{pmatrix} = \begin{pmatrix} \cos(\alpha) & \sin(\alpha) \\ -\sin(\alpha) & \cos(\alpha) \end{pmatrix} \begin{pmatrix} G_{xx} & 0 \\ 0 & G_{yy} \end{pmatrix}$$



Ger de Bruyn

Rotation of the linear polarization angle

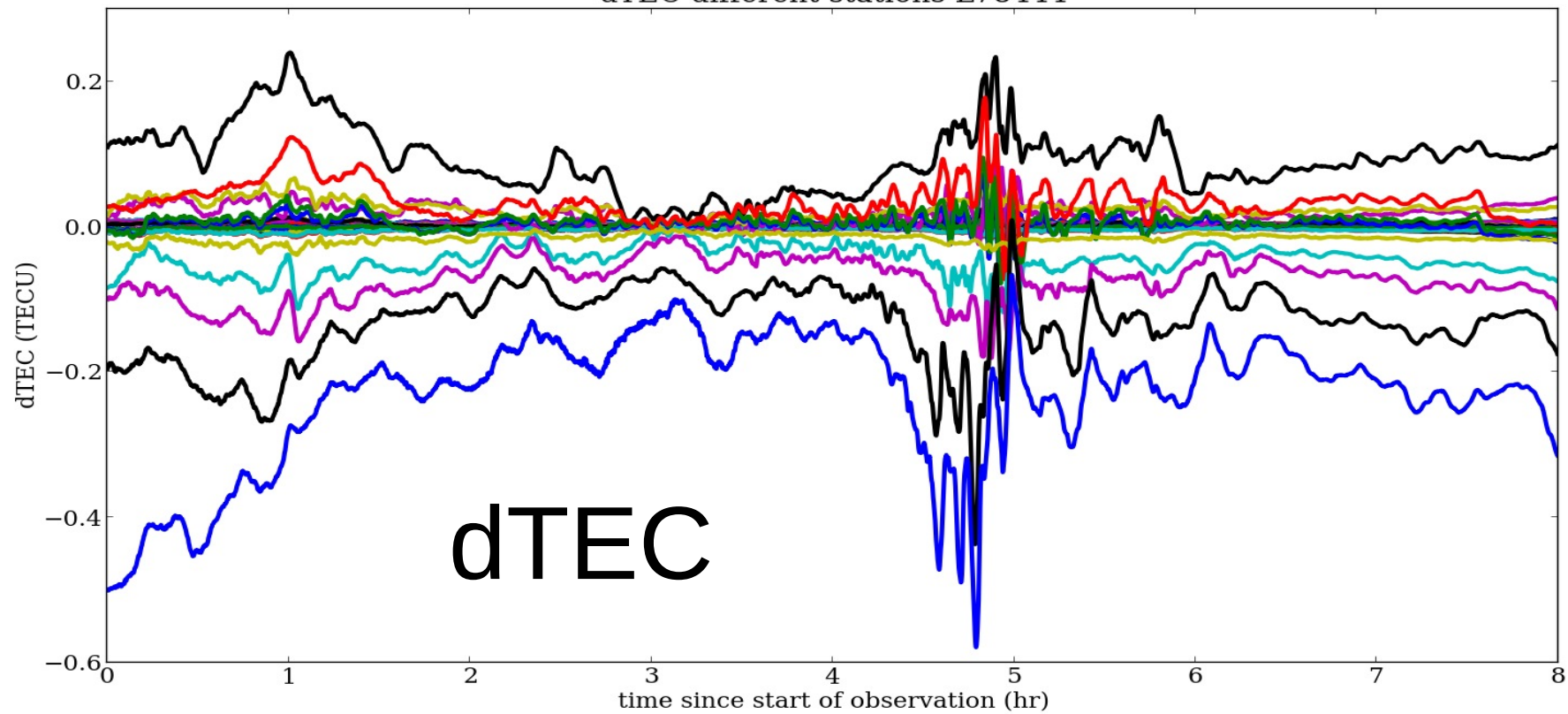
$dRM_{12} \sim TEC_1 * B_{||1} - TEC_2 * B_{||2}$   
 differential RM also for **unpolarized** signal

large TEC gradients: even visible in raw visibilities

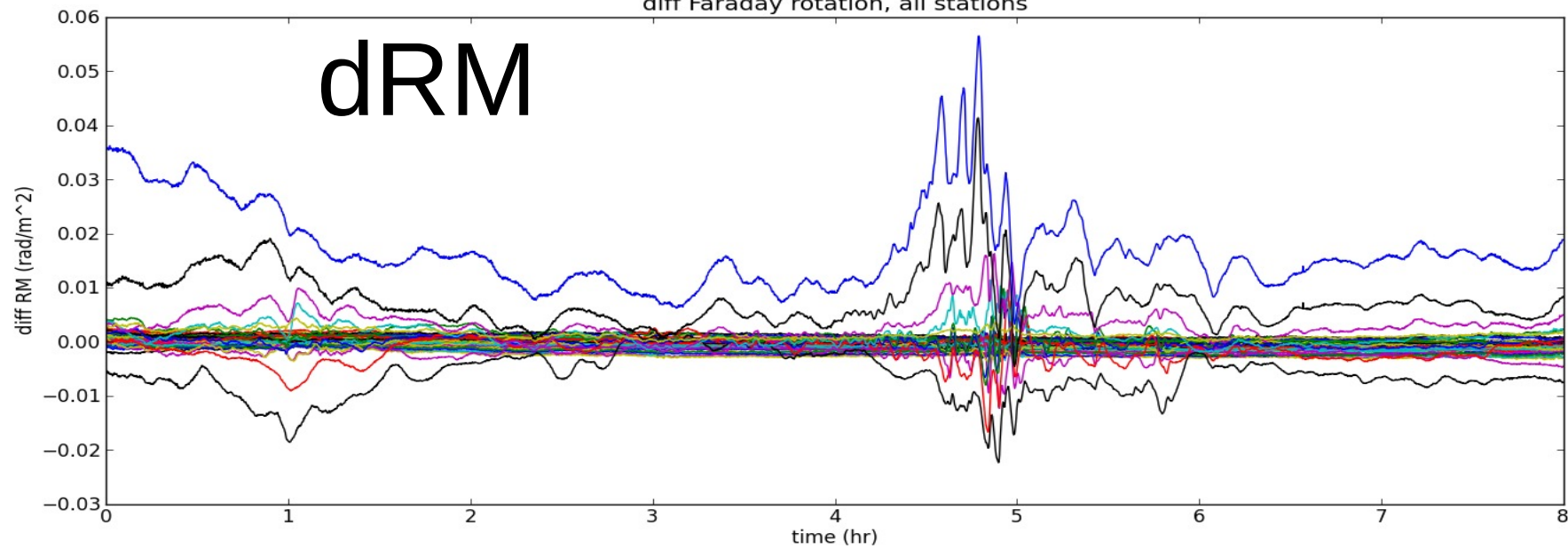
Fit for rotation angle (or extract it from full Jones) per channel.  
 Combine all channels to get dRM



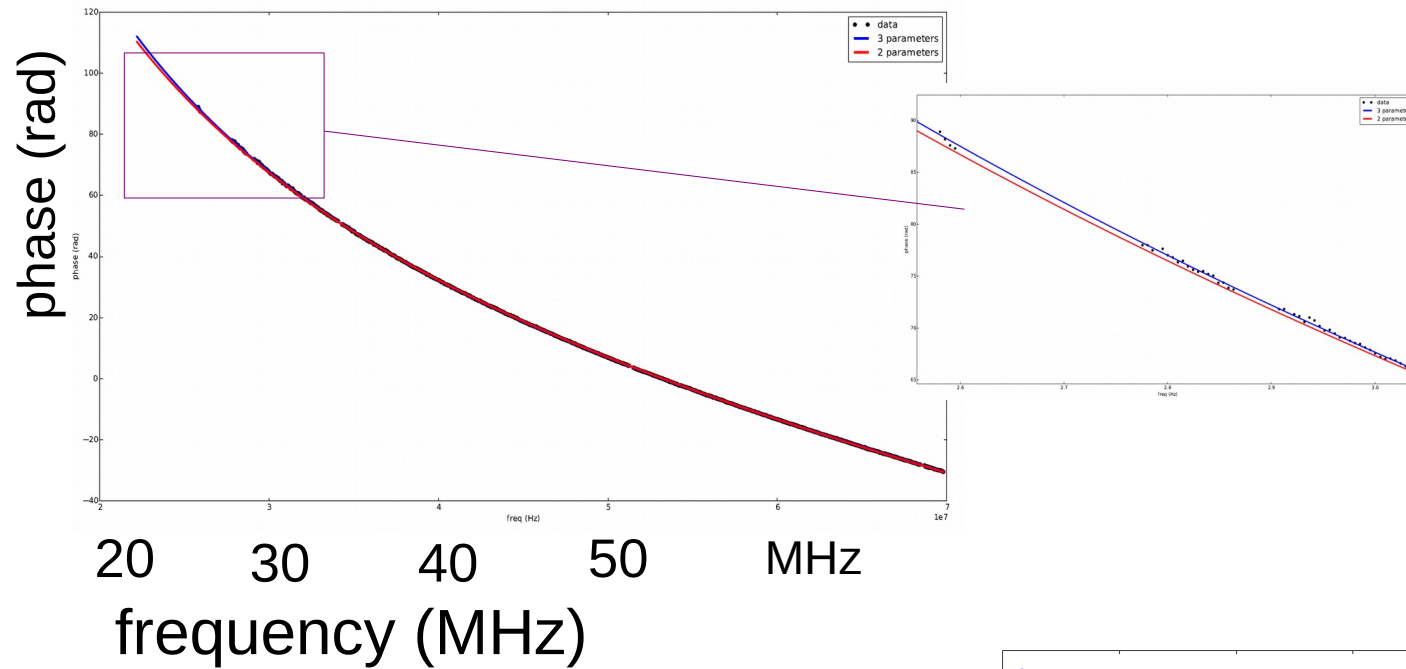
dTEC different stations L78444



diff Faraday rotation, all stations

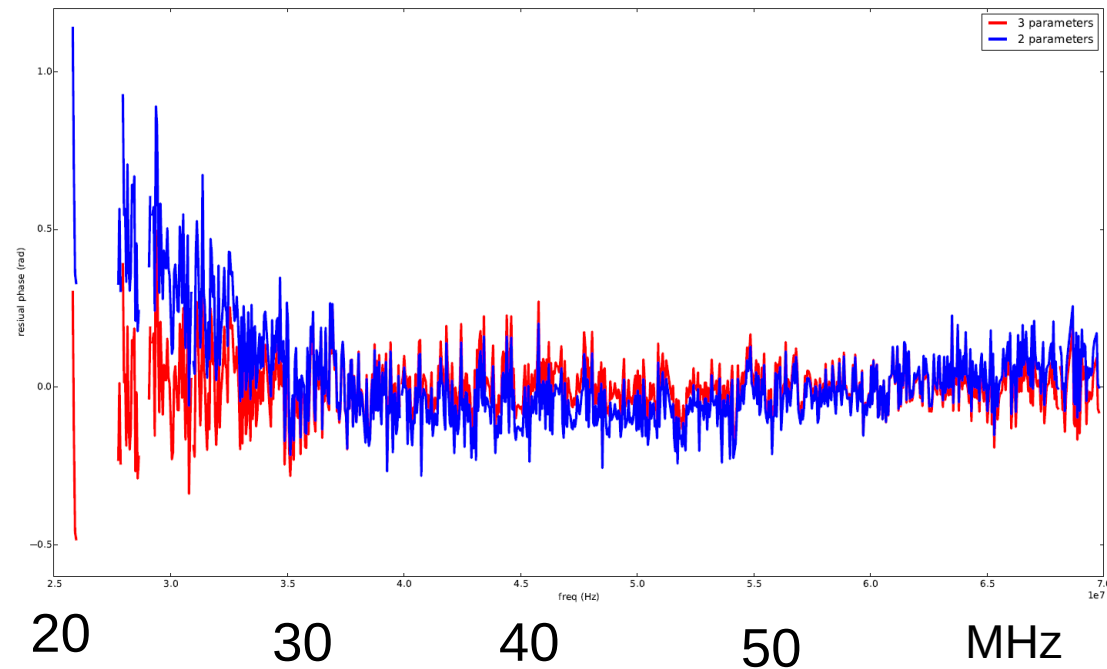


# 3<sup>rd</sup> order



LBA:  
2 parameter  
Clock/TEC fit not  
sufficient for very low  
frequencies (<40 MHz)

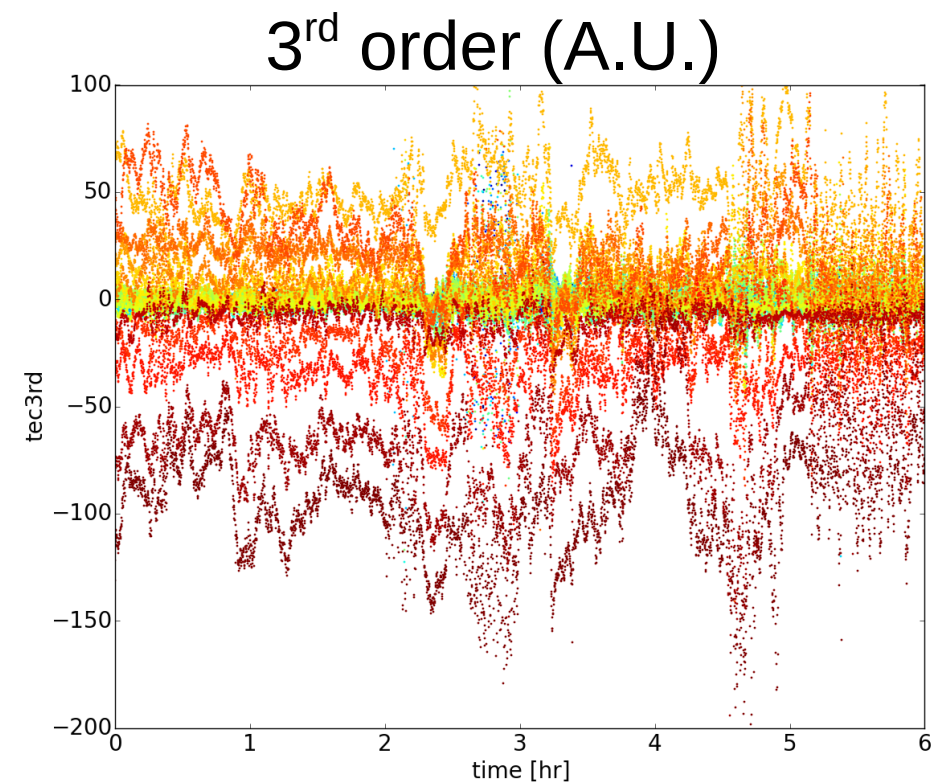
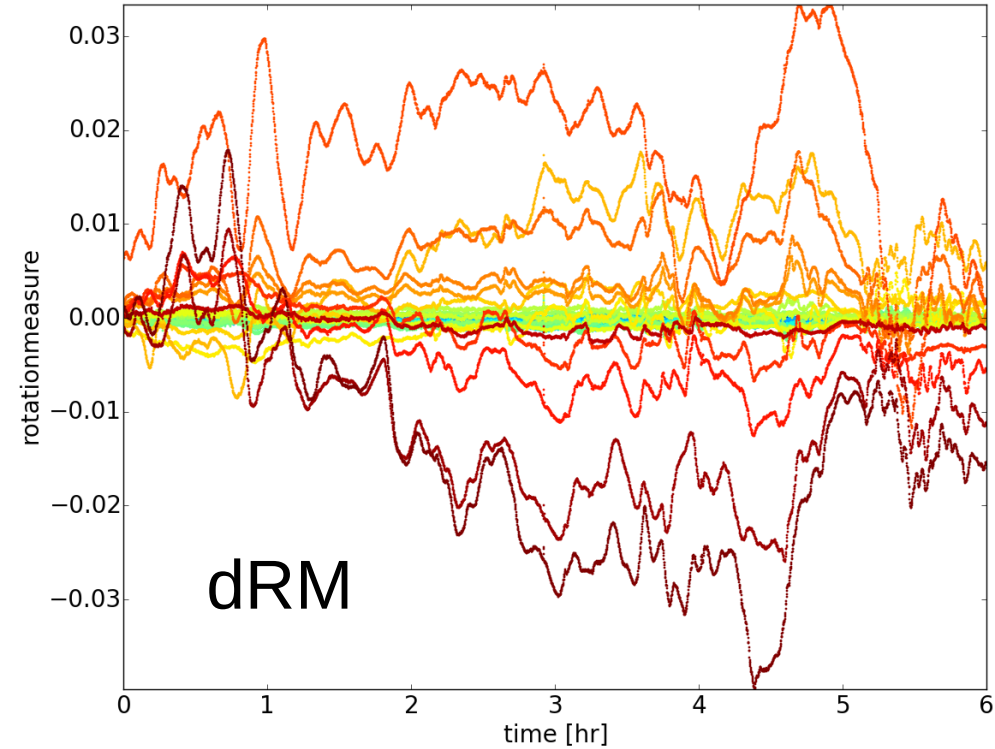
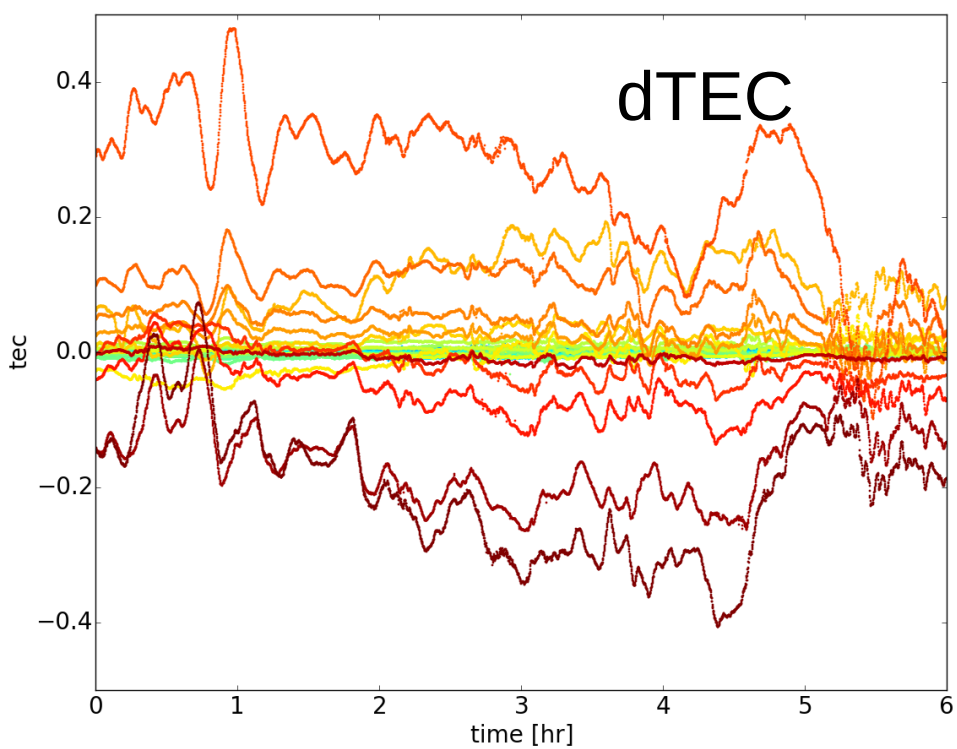
## Residuals



2 parameter fit ( $\varphi(\nu) = A\nu + B/\nu$ )

3 parameter fit ( $\varphi(\nu) = A\nu + B/\nu + C/\nu^3$ )





LBA: dTEC (TECU), dRM (rad/m<sup>2</sup>) and 3<sup>rd</sup> order (arbitrary units) versus time. all stations (F. de Gasperin)

Every dot independent fit!

correlation between stations, correlation between different effects

Combine measurements to extract more information about the underlying structure of the ionosphere. e.g.: 3<sup>rd</sup> order related to  $h_{\max}$

absolute TEC from dRM, B<sub>||</sub> and dTEC

# Structure function

Extract information from dTEC vs. time

Spatial fluctuations:

$$D_{\phi}(\|r_1 - r_2\|) = \langle (\phi_1 - \phi_2)^2 \rangle$$

Kolmogorov turbulence, thin layer approximation:

$$D_{\phi}(\mathbf{r}) = (\mathbf{r} / s_0)^{\beta} \quad \beta = 5/3,$$

$s_0$ : diffractive scale,

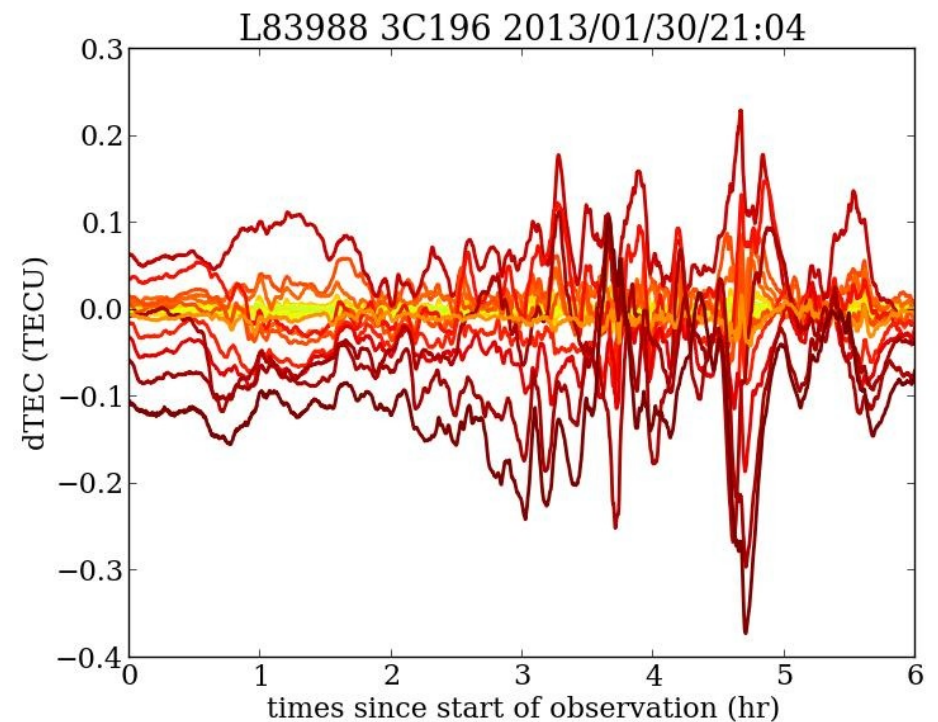
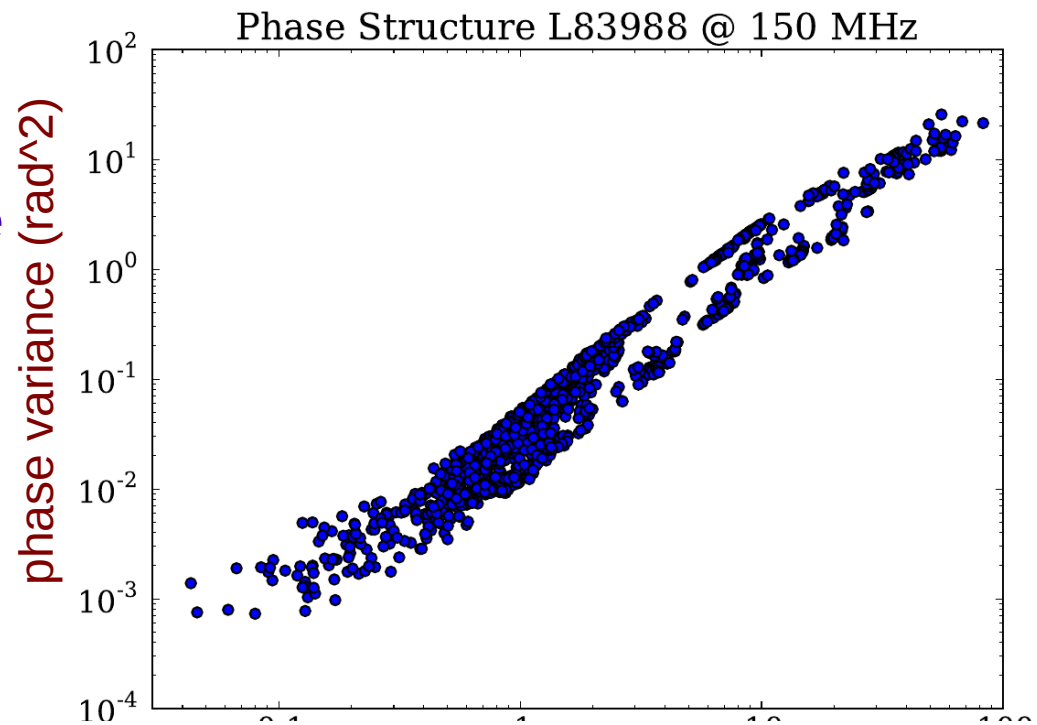
$$D_{\phi}(s_0) = 1 \text{ rad}^2$$

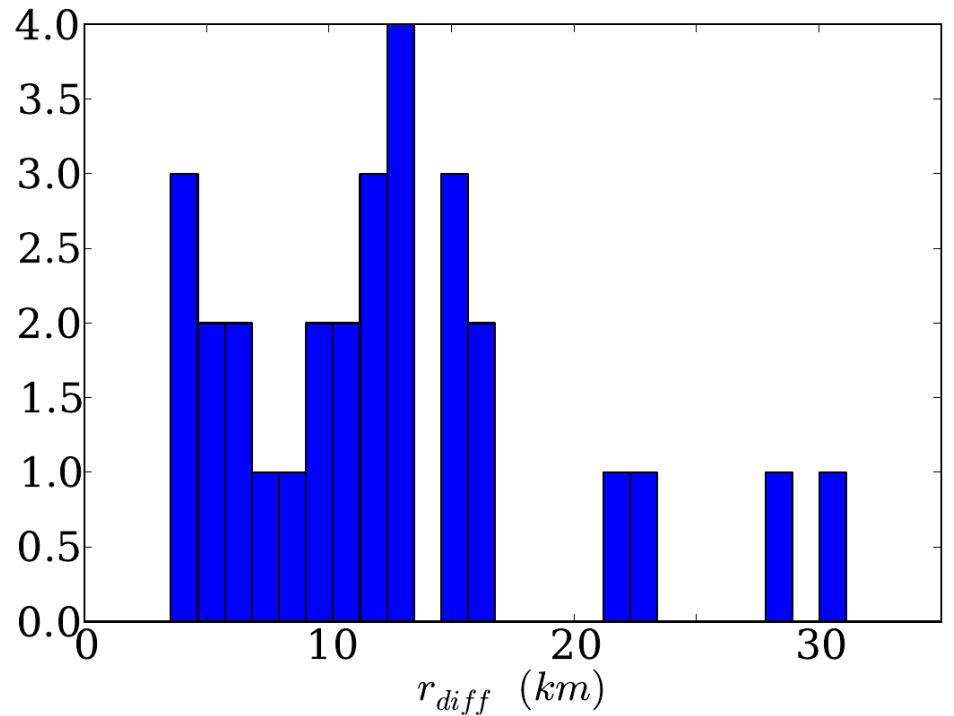
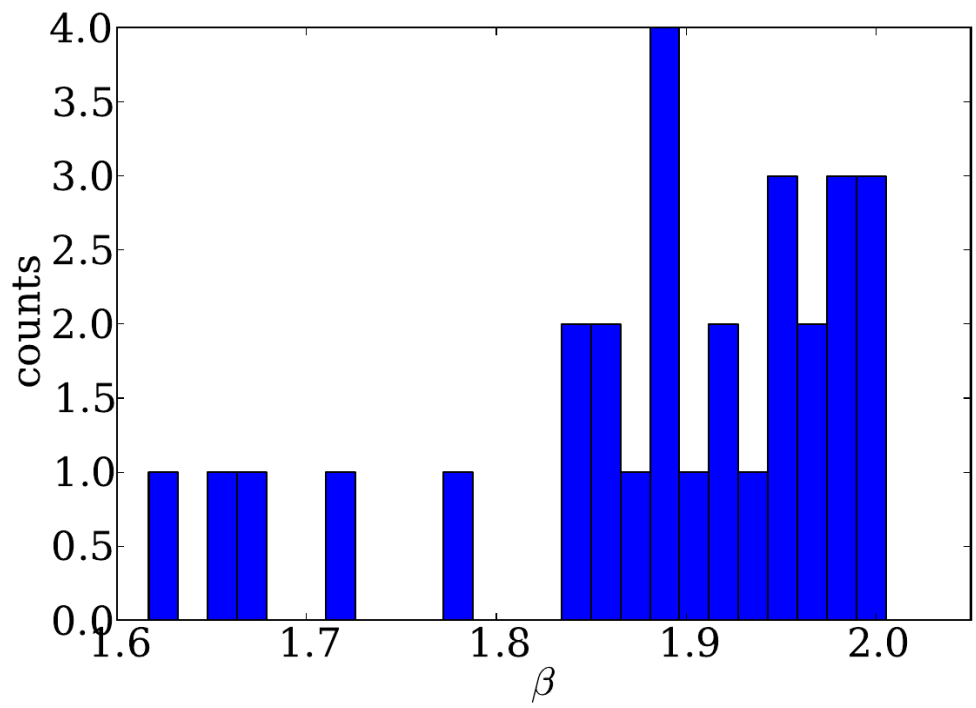
Measure structure function by calculating variance of dTEC vs. time for all baselines

fit  $\beta$ ,  $S_0$

Typical nighttime  $S_0$  @150 MHz: 2-40 km  
scintillation conditions  $S_0 < 2\text{km}$

Characterize ionospheric quality





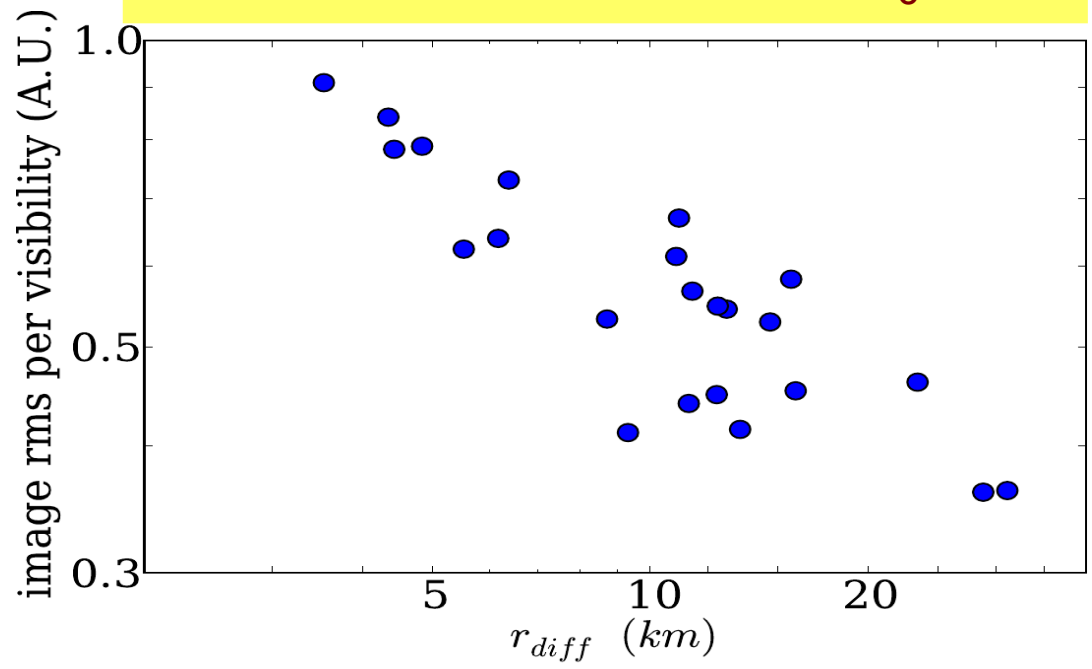
distribution of  $\beta$  and  $r_{diff}$  for 29  
3C196 observations  
nighttime, winter

typically  $\beta$  larger than 5/3  
 $r_{diff}$  varies between 3 and 30 km

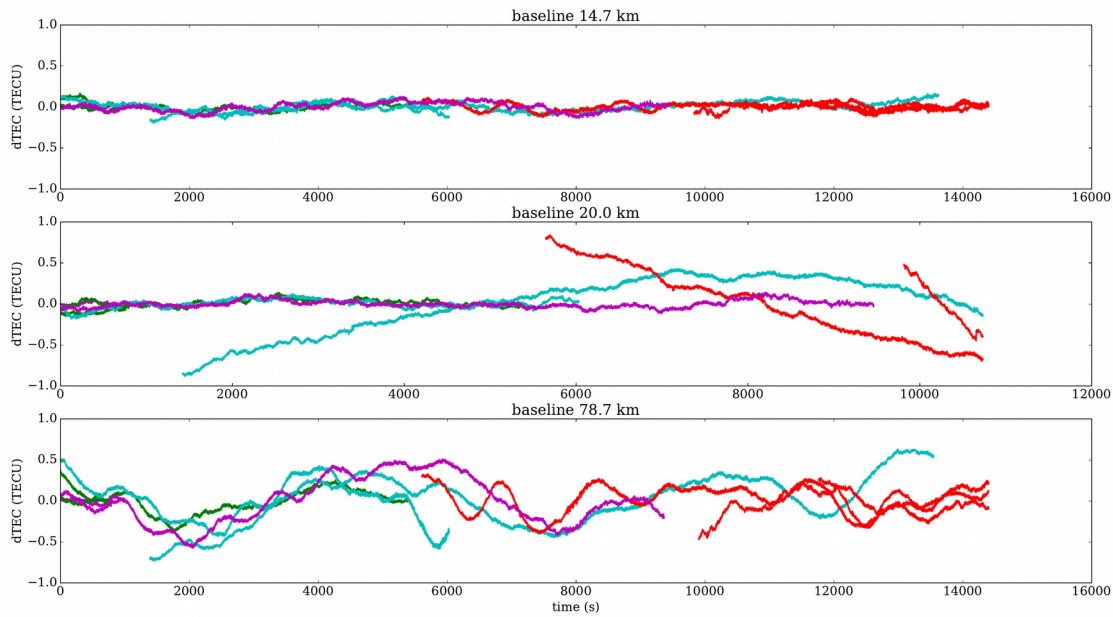
Correlation with image noise after  
DI-calibration only.

baseline length (km)

Correlation image noise  $S_0$



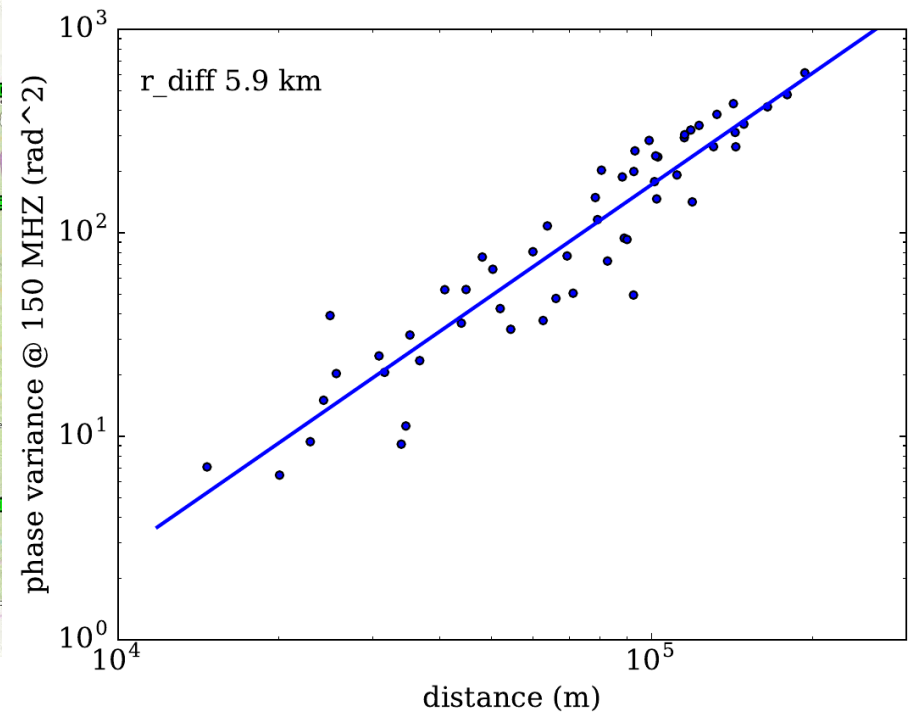
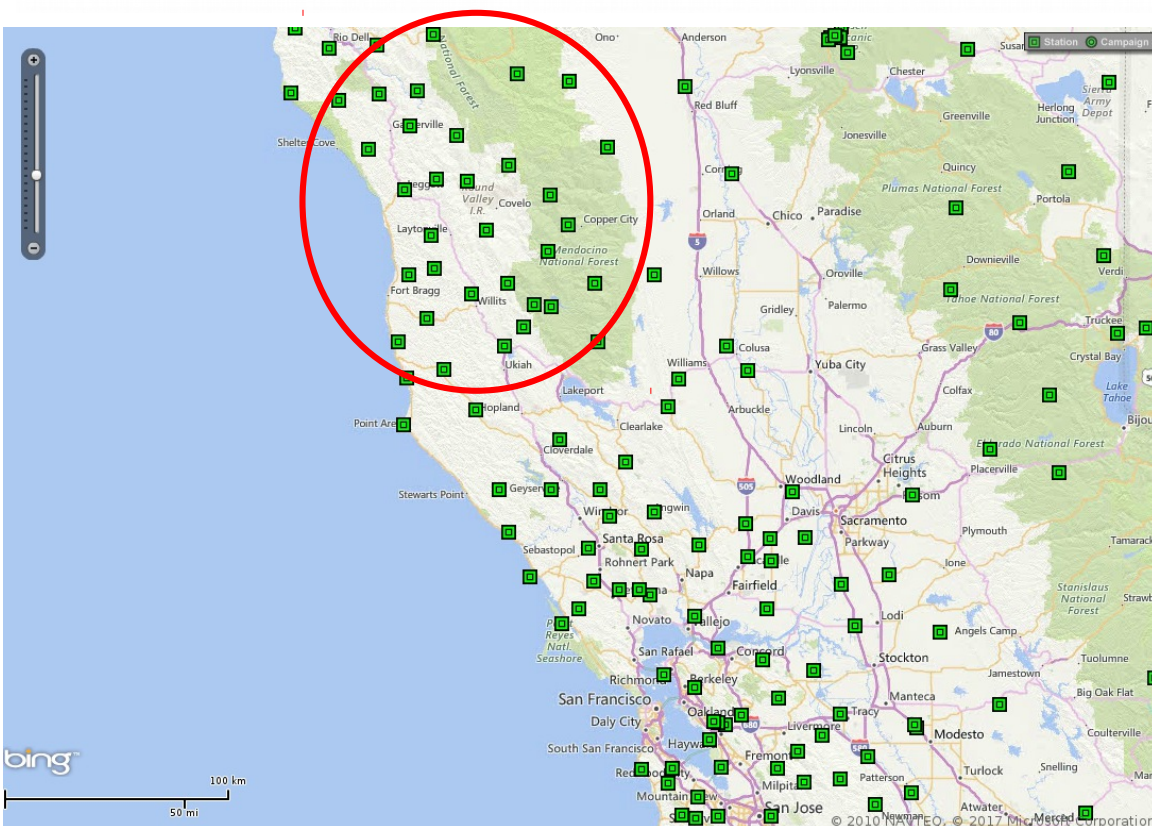




Even possible to extract  $r\_diff$  from high time resolution raw GPS data

Estimate ionospheric quality just before or during observation

Needs dense network of GPS receivers  
(here: public data from several receivers in US-earthquake area)



# Diffractive scale as quality measure

diffractive scale is length scale for which phase variance = 1 rad<sup>2</sup>

(frequency dependent, here @ 150MHz)

correlates with image noise (after DI-calibration)

can be used to assign ionospheric quality to observation:

- discard bad observations
- select very good observations for sky modelling
- determine typical length scale for DD-calibration:
  - number of facets
  - maximum baseline length
- expected scintillation noise after calibration

(e.g. Vedantham and Koopmans (MNRAS 2015))

Easy to obtain from calibration phases, also for non-calibrator fields, without clock-TEC separation and from GPS data

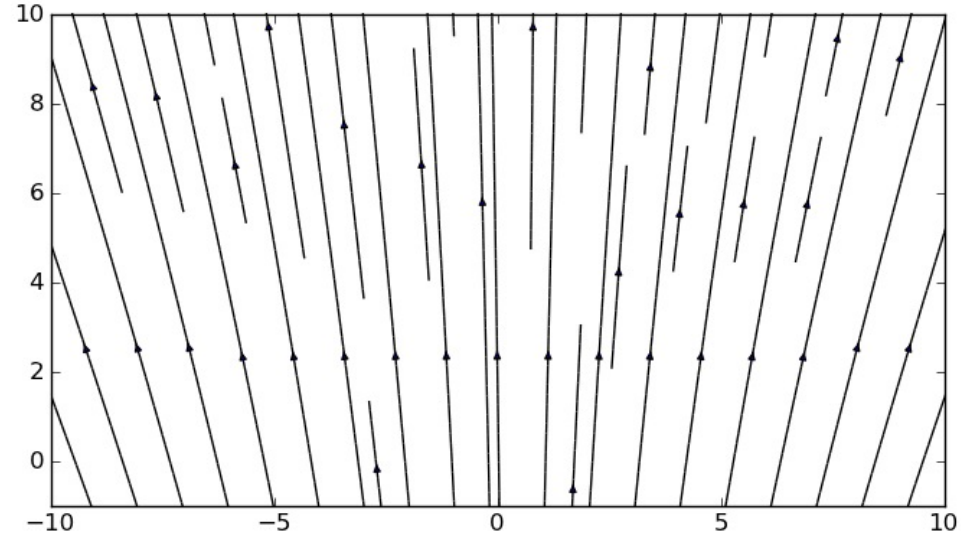


# Large Scale Field Aligned Structure

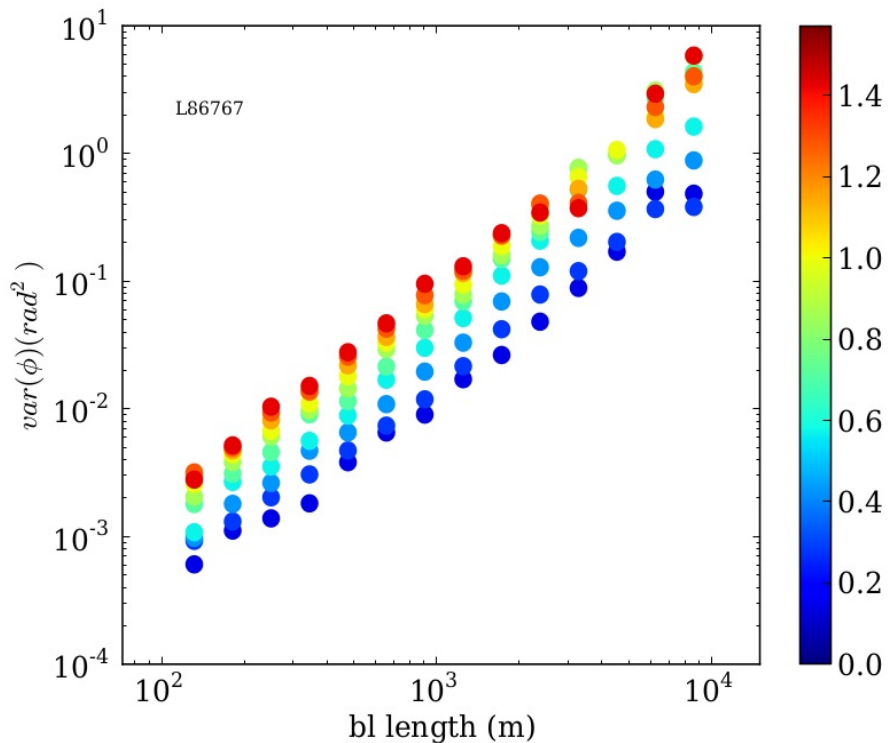
*bandlike* structure → orientation of the baseline

Earth magnetic field aligned?

projected field lines along LOS  
single ionospheric height



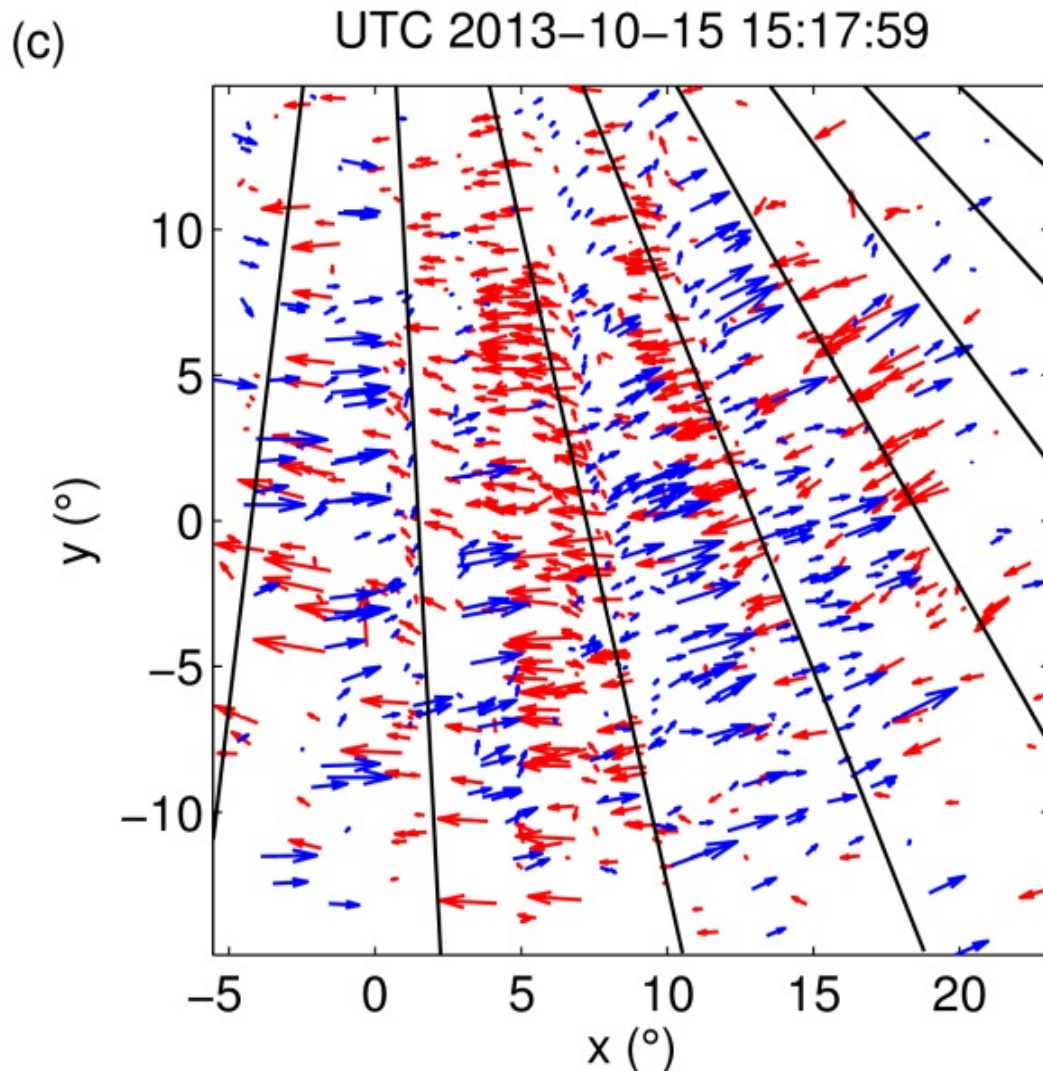
Earth magnetic field lines along viewing angle (NS/EW beam angle, zenith = 0,0)



perspective view → time dependent orientation  
bin data in according to angle  
wrst projected field lines  
field aligned structure observed in ~ 50 % of the observations

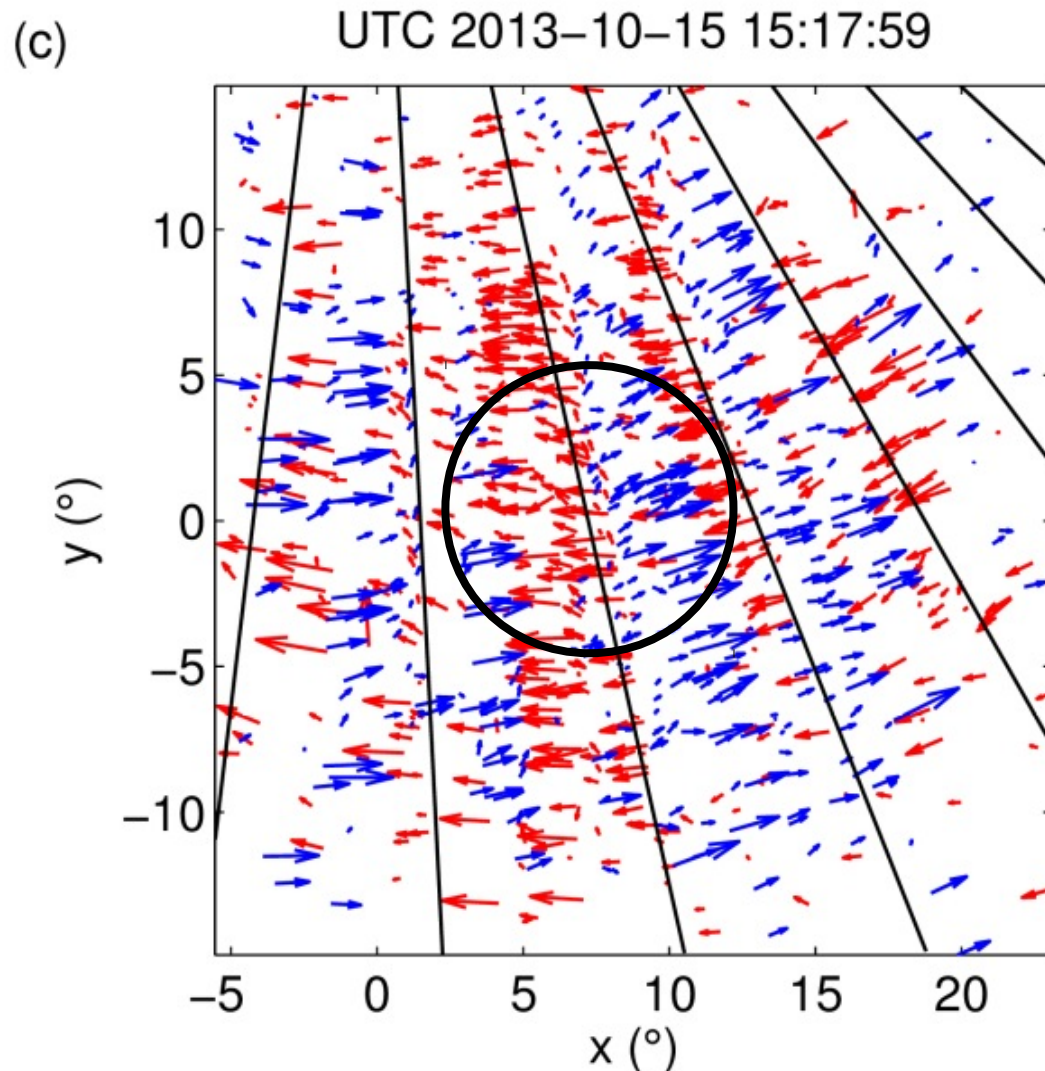
# Loi et al. GRL 2015

## *Real-time imaging of density ducts between the plasmasphere and ionosphere*



MWA data  
snapshot images of  
source shifts  
ionospheric gradient  
→ position shift  
elongated slowly  
moving field aligned  
structures

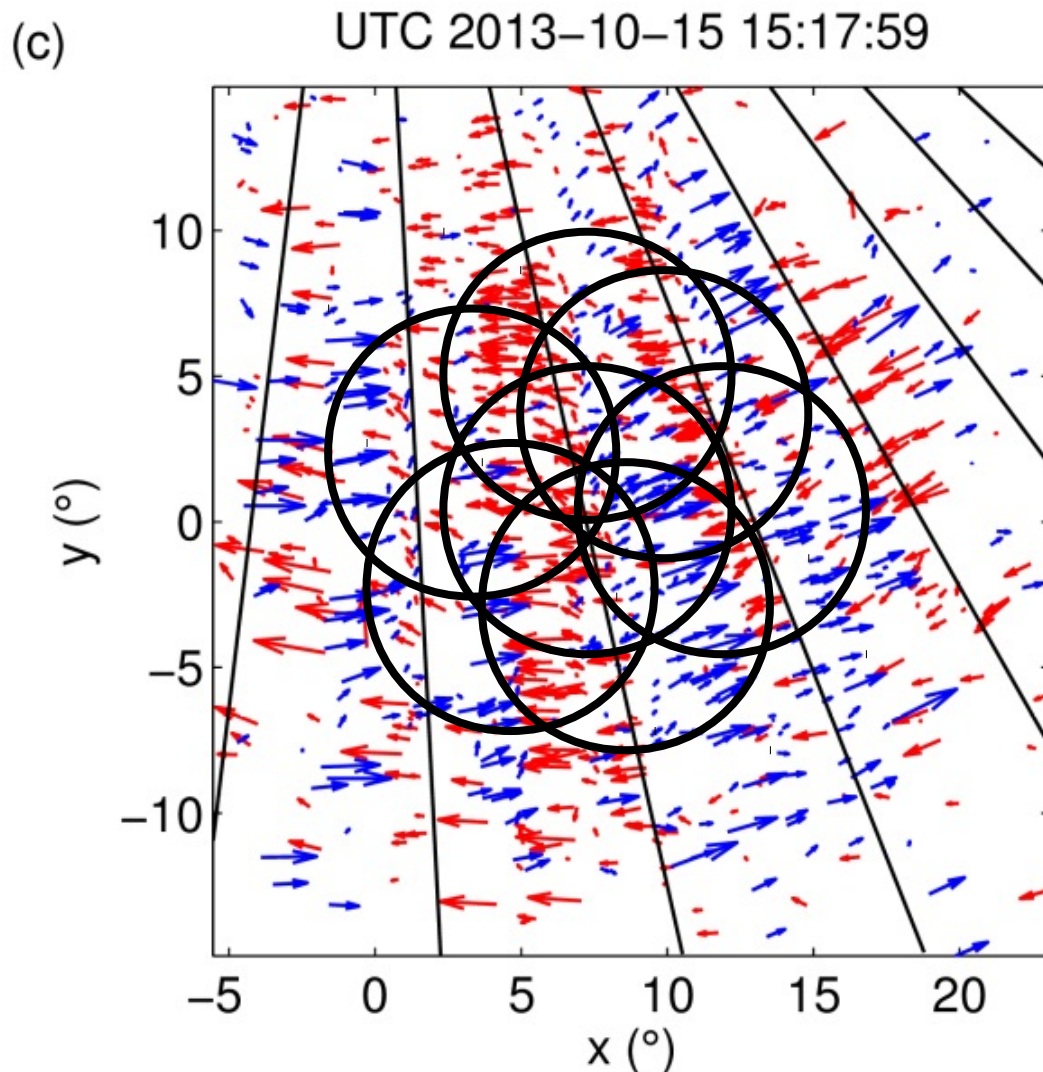
# HBA beam



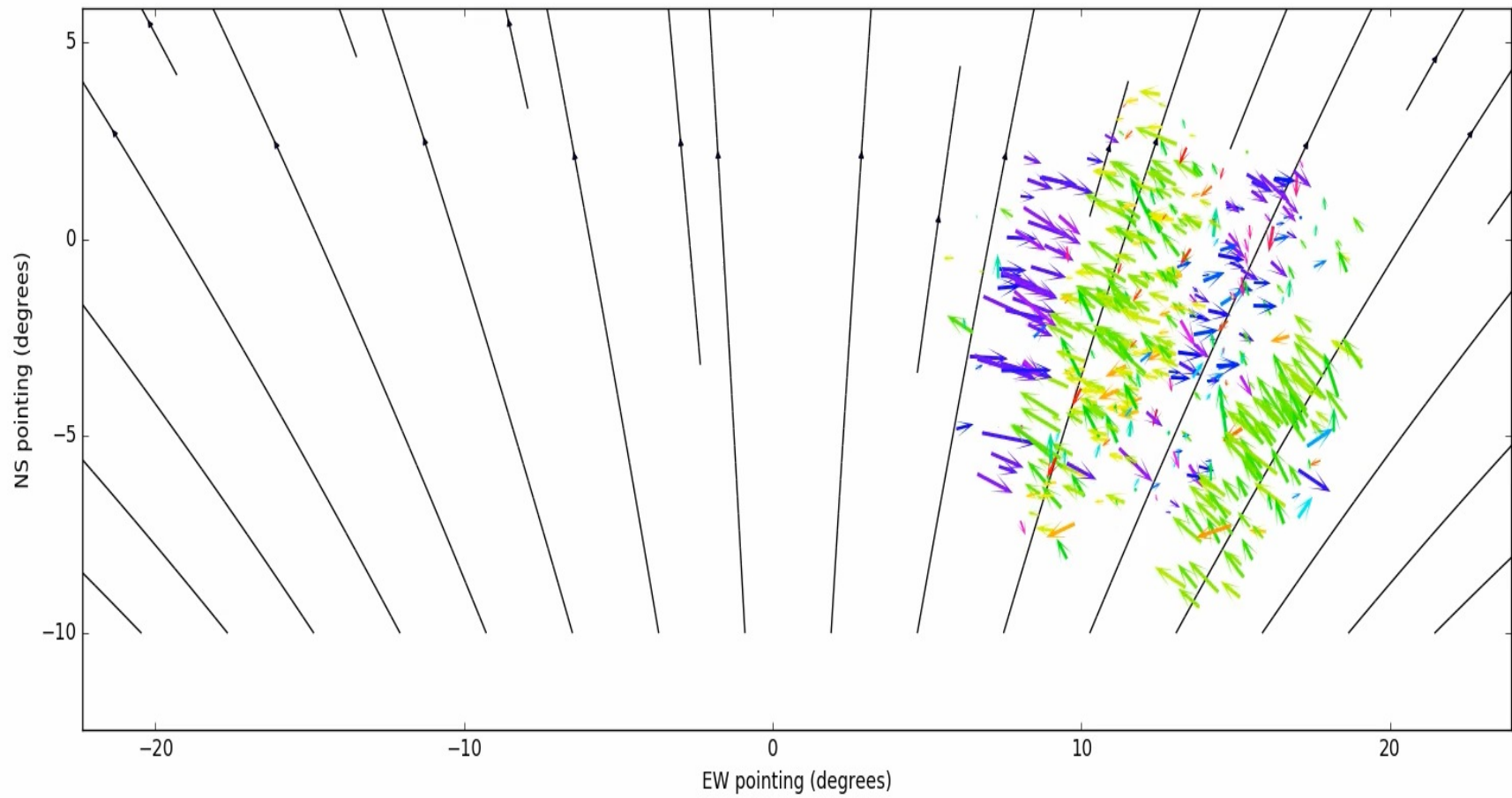
Do we observe the same structures with LOFAR?  
single beam: too small FOV



# flanking fields



Do we observe the same structures with LOFAR?  
single beam: too small FOV  
multiple beams  
standard observing mode for EOR: 1 central beam + 6 flanking fields  
18 SB each  
Use 1min CS only  
snapshot images (wsclean, Offringa) + frequency dependent position fits on ~400 sources





# CONCLUSION

- LOFAR probes ionospheric structures on scales ranges from 100m to 100 km
- Using just calibration gains one gets access to different orders of ionospheric corrutions
- Diffractive scale is a quality measure easily obtained from calibration data
- Anisotropic larger scale magnetic field aligned structures visible in many observations
- Imaging structures using snapshot views from core only data (multibeaming)